2016

Assessing the Sensitivity of the Non-Hydrostatic Regional Climate Model to Boundary Conditions and Convective Schemes over the Philippines

Gemma T. Narisma

Faye T. Cruz

Hidetaka Sasaki

Journal of the Meteorological Society of Japan, Vol. 94A, pp. 165−179, 2016
DOI:10.2151/jmsj.2015-059

Assessing the Sensitivity of the Non-Hydrostatic Regional Climate Model to Boundary Conditions and Convective Schemes over the Philippines

Faye T. CRUZ

Manila Observatory, Ateneo de Manila University Campus, Quezon City, Philippines

Hidetaka SASAKI

Atmospheric Environment and Applied Meteorology Research Department, Meteorological Research Institute, Tsukuba, Japan

and

Gemma T. NARISMA

Manila Observatory, Ateneo de Manila University Campus, Quezon City, Philippines
Atmospheric Science Program, Physics Department, Ateneo de Manila University, Quezon City, Philippines

(Manuscript received 11 November 2014, in final form 3 October 2015)

Abstract

Regional climate models have been useful in climate studies and in downscaling climate projections from global climate models, especially for areas characterized by complex topography and coastline features, such as the Philippines. However, several factors may affect model skill, such as uncertainties related to the boundary conditions and model configuration. This study evaluates the performance of the non-hydrostatic regional climate model (NHRCM) over the Philippines. Present-day climate simulations at 50 km resolution are conducted using two sets of boundary conditions (ECMWF ERA-Interim and the NCEP/NCAR Reanalysis Project NNRP1), as well as two convective parameterization schemes in the model (Grell and Kain-Fritsch). Results show that the seasonal changes in the spatial distribution of temperature, rainfall, and winds over the Philippines are simulated reasonably well. NHRCM has an overall cold and dry bias over land, the degree of which depends on the boundary condition and the convective scheme used. After adjusting the simulated temperature because of the difference in topography, the temperature differs from that observed by −0.90°C to −0.42°C on average. The rainfall bias in NHRCM ranges from −62.13 % to −25.20 %. Regardless of the boundary condition, the Grell scheme results in the lowest temperature bias with high skill scores, while the Kain-Fritsch scheme gives the lowest rainfall bias with high correlation and skill scores. The boundary conditions also influence model skill, such that the model bias is lower for temperature when ERA-Interim is used, but lower for rainfall with NNRP1. NHRCM represents the seasonal cycles of temperature and rainfall for all regions, but tends to generate more occurrences of cold and dry months. Improvements in the model are still possible, but these results indicate the potential of the model to be used for providing essential information for describing historical and future changes in the Philippine climate.

Keywords regional climate model; Philippine climate; model evaluation

Corresponding author: Faye T. Cruz, Manila Observatory, Ateneo de Manila University Campus, Loyola Heights, Quezon City 1108, Philippines
E-mail: fcruz@observatory.ph

1. Introduction

The exposure of the high population of the Philippines to climate-related hazards places the country at risk to the impacts of climate change, which is further aggravated by its low adaptive capacity. In particular, according to the World Risk Report, the Philippines has been ranked third in the list of countries with high risk to the impacts of climate change since 2011 and is currently ranked second after Vanuatu as of 2014 (see http://www.weltrisikobericht.de/Bericht.435.0.html?&L=3, accessed November 5, 2014). The country's vulnerability has been emphasized recently with the devastation caused by Typhoon Haiyan in 2013, the heavy rainfall events associated with monsoons and tropical cyclones that have resulted in intense flooding in Mindanao in 2011 due to Tropical Storm Washi, and in metropolitan Manila in 2012 and 2013 due to the enhanced southwest monsoon rainfall. Prolonged dry conditions also threaten agricultural production as indicated by declines in rice production during El Niño events (Roberts et al. 2009; Villarin and Narisma 2011). Climate projections under a globally warmer world indicate significant changes in mean temperature and precipitation with increased extreme weather events by the end of the 21st century. High-resolution climate information is therefore vital in order to prepare sound strategies and policies to adapt and respond to the potential impacts of these climate-related hazards.

Global climate models (GCM) have been useful tools to provide climate information from the past, near present, and future, which are needed to prepare for the potential impacts of future changes in the global climate. However, GCMs have coarse spatial resolutions, typically ranging from 100 to 250 km, which may be inadequate to resolve some features of the regional climate. Particularly for archipelagic regions like the Philippines, topography, land use, and coastlines need to be properly represented in the model since these affect climate at the local scale. Downscaling methods can be used, whether statistical or dynamical (i.e., using a regional climate model (RCM)), to obtain higher-resolution climate information from GCMs for a particular region, wherein each method would have its own advantages and disadvantages (Robertson et al. 2012).

Studies have shown that RCMs can provide added value to GCMs, especially for areas with complex topography and coastlines (Feser et al. 2011). In the Philippines, RCMs have been used to examine historical climate and for downscaling climate projections (e.g., Im et al. 2008; Robertson et al. 2012). For example, the Abdus Salam International Centre for Theoretical Physics Regional Climate Model version 3 (RegCM3) was used to examine the summer monsoon precipitation over the country and the model sensitivity to lateral boundary conditions and ocean flux schemes (Francisco et al. 2006). Recently, this model was also used to provide wind fields for an assessment of wind-energy projection over a wind farm site in the Philippines (Silang et al. 2014). In addition, other RCMs such as the UK Met Office Hadley Centre Providing Regional Climates for Impacts Studies (PRECIS) model and the Weather Research and Forecasting (WRF) model have been used to project future changes in temperature and rainfall over the Philippines and in Southeast Asia (Philippine Atmospheric, Geophysical and Astromical Service Administration (PAGASA) 2011; Chotamonsak et al. 2011).

In this study, the performance of another RCM, the non-hydrostatic regional climate model (NHRCM), is examined in simulating the local climate of the Philippines. Previous studies have shown the capability of NHRCM in simulating the present climate of Japan (Sasaki et al. 2008, 2011). This study therefore aims to evaluate the model in simulating the near-recent climate of the Philippines before it will be used to further investigate processes influencing its local climate, as well as in downscaling climate projections. Section 2 describes the numerical experiments conducted and the methodology for the analysis of model output. Results of the model evaluation are discussed in Section 3. Finally, Section 4 lists a summary of the key findings.

2. Methodology

2.1 Description of the numerical experiment

Simulations have been done using the NHRCM (Sasaki et al. 2008), a regional climate model based on the non-hydrostatic model developed at the Meteorological Research Institute (MRI) and the Numerical Prediction Division of the Japan Meteorological Agency (JMA) (Saito et al. 2006). In this model, the land surface is represented by the MRI−JMA Simple Biosphere model (Hirai and Ohizumi 2004). NHRCM also includes a spectral nudging scheme based on the spectral boundary coupling method of Kida et al. (1991) and Sasaki et al. (2000), which tries to preserve the large-scale field (long-wave component) of the boundary condition within the nested inner domain in wavenumber space (Nakano et al. 2012), and consequently results in improved model perfor-

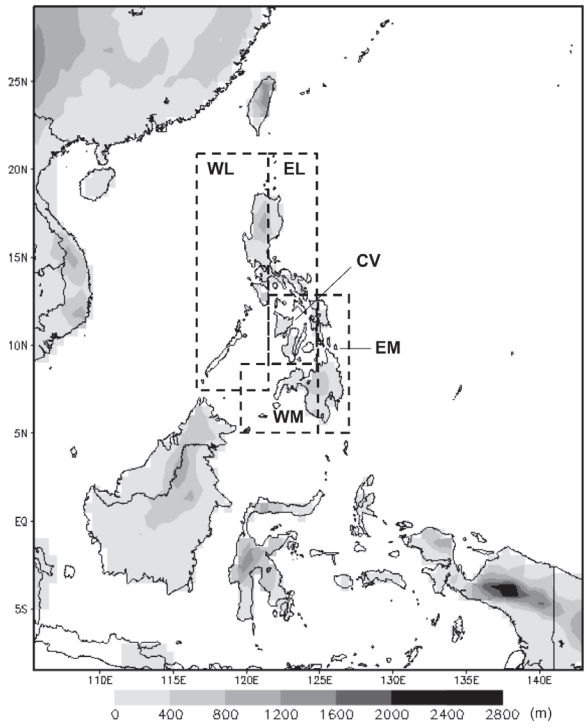

Fig. 1. Map of the simulation domain with subregions: West Luzon (WL), East Luzon (EL), Central Visayas (CV), West Mindanao (WM), and East Mindanao (EM). The terrain elevation (m, shaded) is shown over areas where land fraction is greater than 50 %.

mance (Yasunaga et al. 2005).

Figure 1 shows the domain centered over the Philippines at a 50-km resolution using a Mercator map projection. Using 50 vertical layers, the model is run for 10 years, starting from April 1998 to May 2008, at a time step of 60 seconds. Each year is run in parallel such that each run consists of 14 months beginning from April. The first two months are discarded such that the analysis is focused from June to May of the following year.

The model performance may be affected by several factors such as the boundary conditions and the parameterization schemes used in the model (e.g. Fersch and Kunstmann 2014; Park et al. 2013). Thus, sensitivity tests have been conducted using two global driving reanalyses: ECMWF ERA-Interim (Dee et al. 2011), and NCEP/NCAR Reanalysis Project (NNRP1; Kalnay et al. 1996; Kistler et al. 2001). Although the native horizontal spatial resolution of the ERA-Interim dataset is ~79 km, the resolution of the driving dataset used in this study is ~222 km, which is closer to the ~209-km spatial resolution of the NNRP1 dataset. In addition, two cumulus convective parameterization schemes in the model were tested: Grell (Grell 1993) and Kain-Fritsch (Kain and Fritsch 1993; Ohmori and Yamada 2004; Yamada 2003). Preliminary runs using the Kain-Fritsch scheme showed that rainfall tends to be overestimated, especially over the ocean. In order to address this issue, one of its parameters, del_abe, was changed from its default value of 0.15 to 0.3. This parameter is related to the closure assumption of the Kain-Fritsch scheme, which sets the amount of the existing convective available potential energy (CAPE) that remains after convection (Ohmori and Yamada 2004). Thus, increasing this parameter decreases the consumption of CAPE, and consequently weakens the effects of the cumulus parameterization. Table 1 lists the experiments in this study, which includes the names that will be referred to here.

2.2 *Numerical analysis*

For the model evaluation, gridded observation datasets have been used to overcome limitations posed by sparse meteorological stations and missing data. Temperature and rainfall data are obtained from the 0.5° resolution Asian Precipitation–Highly Resolved Observational Data Integration Towards Evaluation (APHRODITE) project, i.e. AphroTemp_V1204R1 and APHRO_MA_V1101R2, respectively (Yasutomi et al. 2011; Yatagai et al. 2009, 2012; downloaded from http://www.chikyu.ac.jp/precip). These datasets are based on station records as well as pre-compiled datasets, and are available only over land. To characterize the rainfall seasonality over ocean, rainfall information from the Tropical Rainfall Measuring Mission (TRMM 3B43 version 7; Huffman et al. 2007) at 0.25° resolution was also used in this study. Since the TRMM dataset begins only from January 1998 and the APHRODITE dataset ends in December 2007, the time period selected for the analysis of model results is from June 1998 to May 2007.

The monthly mean 1.5 m temperature and rainfall from the model are evaluated with respect to the gridded observation datasets. Differences in height between actual and model elevation can affect the simulated temperature. Thus, the model values (over land points only) have been adjusted using a temperature lapse rate of 6 °C km^{-1}, similar with APHRODITE (Yasutomi et al. 2011). Terrain elevation data at 0.5° resolution is obtained from the Global 30

Table 1. List of model experiments.

Experiment Name	Boundary Condition	Convective Scheme
NHRCM_ERA_KF	ERA-Interim	Kain-Fritsch (with del_abe=0.3)
NHRCM_ERA_GR	ERA-Interim	Grell
NHRCM_NNRP1_KF	NNRP1	Kain-Fritsch (with del_abe=0.3)
NHRCM_NNRP1_GR	NNRP1	Grell

Arc-Second Elevation Data Set (GTOPO30) accessed using the Spatial Data Access Tool of the Distributed Active Archive Center for Biogeochemical Dynamics of the Oak Ridge National Laboratory (ORNL DAAC; Wei et al. 2009). The difference in the terrain heights is determined per land grid point and used for the temperature correction.

Key features to be examined in the model simulations include the seasonality, magnitude, and spatial distribution of temperature and rainfall in the Philippines. Five subregions have also been identified: West Luzon (WL), East Luzon (EL), Central Visayas (CV), West Mindanao (WM), and East Mindanao (EM), which encompass only the big islands of the Philippines given the resolution used in this study (see Fig. 1). These regions have been divided according to the three main island groups: Luzon, Visayas, and Mindanao, and further subdivided to group areas having similar climate characteristics, e.g., part of Eastern Visayas is grouped here with East Mindanao. For the regional analysis, only values over land will be used. These areas are identified in the model where land fraction is greater than 50 %.

The model's skill is examined for each region, particularly in capturing the seasonal cycle and frequency distribution using the probability density function for monthly mean temperature, and histogram for monthly total rainfall. Performance measures such as bias and correlation values are also derived. A skill score based on Perkins et al. (2007) is used to measure the closeness of the frequency distributions between observed and model output. It is defined here as follows:

$$\text{skill score} = \sum_{i=1}^{n} \text{minimum}\left(\frac{f_i(o)}{N(o)}, \frac{f_i(m)}{N(m)}\right), \qquad (1)$$

where $f_i(o)$ and $f_i(m)$ are the frequency distributions of the observed and model values, respectively, normalized by their corresponding total number of samples N (particularly for the rainfall histograms) for each bin i, and n is the number of bins. Table 2 lists the values of N. The skill score describes the common area or overlap between the two distributions by taking the sum of the minimum of the two normalized distributions at each bin. The skill score ranges from zero to one, such that a score of one indicates the superior skill of the model in capturing the distribution of the observed values.

Table 2. Number of samples (N) used in calculating the skill score for the rainfall frequency distribution (histogram), which consists of monthly values over land grid points within each subregion, and over the Philippines.

Region	APHRODITE	NHRCM
WL	7452	2376
EL	3996	1512
EM	4104	1836
CV	5292	1188
WM	4536	1512
PH	25380	8424

3. Results and discussion

3.1 Seasonal means

a. Temperature

The climate of the Philippines is described as tropical and maritime. During the summer season from June to August (JJA), the temperature over the country averages about 28°C with cooler temperatures over the mountainous areas in northwest of Luzon island and western section of Mindanao island (Fig. 2a). Figs. 2b and 2e show that both driving reanalyses data at their respective resolutions tend to be warmer compared to the observed temperature (Fig. 2a). This is likely due to having very few land points over the domain because of their coarse spatial resolution. When downscaled with NHRCM, topography is better represented, which affects the simulated temperature, e.g., the lower temperature over the mountains (Figs. 2c, d, f, g). Comparison of the runs indicates that the convective schemes have minimal effect on simulated temperatures, regardless of the boundary condition,

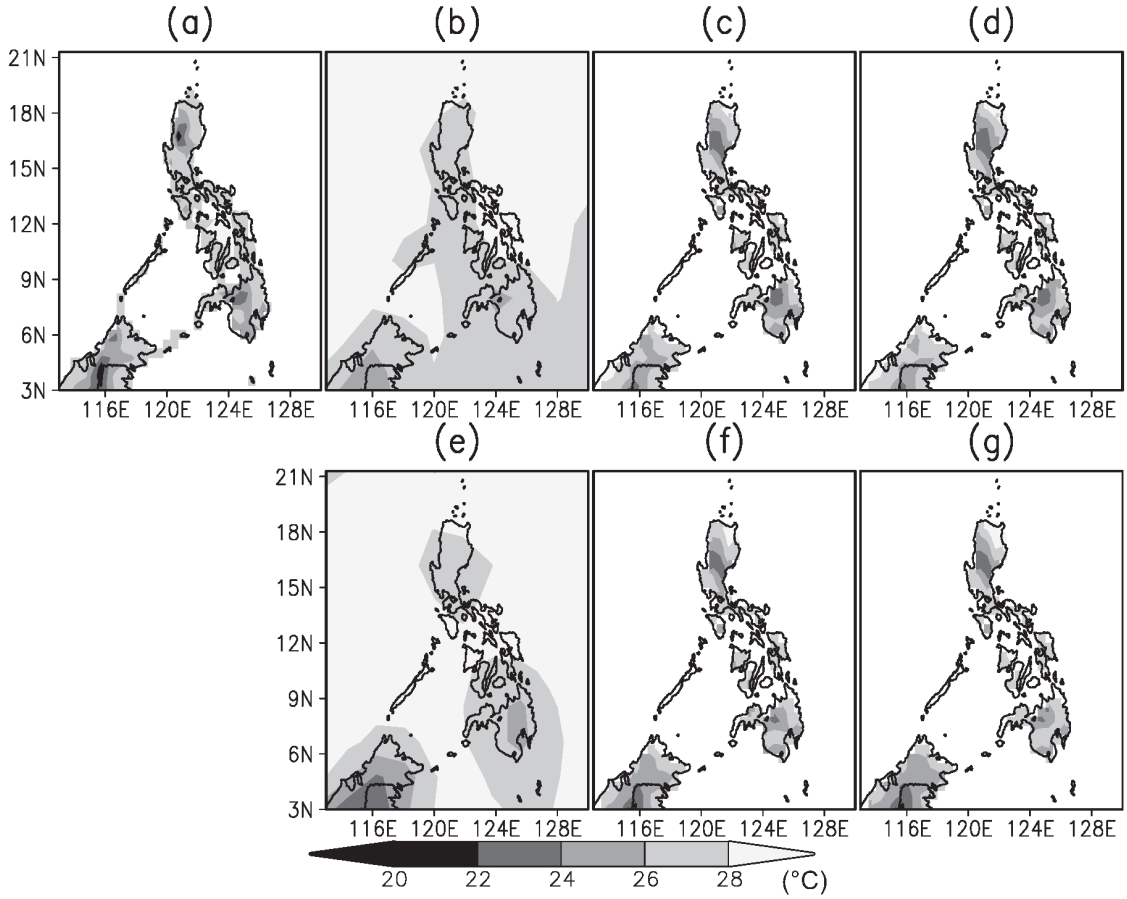

Fig. 2. Average seasonal temperature (°C) from June to August from (a) APHRODITE, (b) ERA-Interim, (c) NHRCM_ERA_KF, (d) NHRCM_ERA_GR, (e) NNRP1, (f) NHRCM_NNRP1_KF, and (g) NHRCM_NNRP1_GR. Only the values over land are shown for APHRODITE and NHRCM.

given the similarity in spatial patterns and magnitude (see Figs. 2c, d, f, g).

Most areas in the country have temperatures of about 24°C–28°C during the cooler months of December to February (DJF) (Fig. 3a). Both ERA-Interim and NNRP1 show relatively higher temperatures over the domain, which is mostly identified as ocean (Figs. 3b, e). Regardless, NHRCM generates a spatial distribution close to APHRODITE (Figs. 3c, d, f, g), albeit cooler over the mountain region in Luzon island, similar to JJA. During this season, the influence of the convective schemes is also minimal (Figs. 3f, g).

b. Rainfall

The seasonal and spatial variability in the Philippine climate is mainly driven by rainfall, which is influenced by both local processes and large-scale systems, e.g., the northeast and southwest monsoons, tropical cyclones, and the El Niño Southern Oscillation (Cruz et al. 2013; Villafuerte et al. 2014). In JJA, the southwest monsoon brings abundant rainfall over the western coast, particularly over northwest Luzon, while the rest of the country receive at least 5 mm day^{-1} (Figs. 4a, e). Compared with NNRP1, ERA-Interim better captures the rainfall distribution, particularly its west to east gradient over the country, but both reanalyses underestimate the observed rainfall amount at their coarse spatial resolution (Figs. 4b, f). NHRCM captures the southwest monsoon and its associated high rainfall along the western coastline. However, the model underestimates rainfall along the eastern coast and tends to be drier than ERA-Interim and NNRP1 over the rest of the country (Figs. 4c, d,

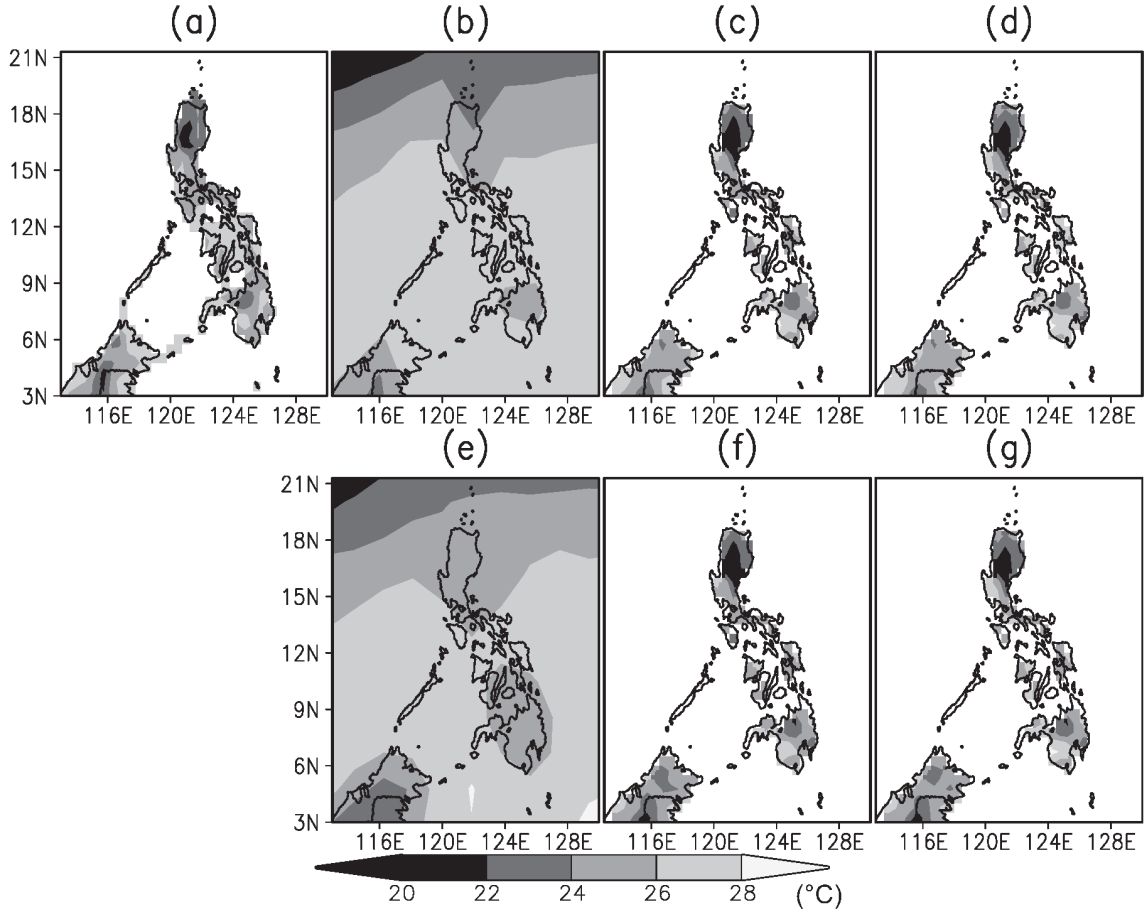

Fig. 3. Average seasonal temperature (°C) from December to February from (a) APHRODITE, (b) ERA-Interim, (c) NHRCM_ERA_KF, (d) NHRCM_ERA_GR, (e) NNRP1, (f) NHRCM_NNRP1_KF, and (g) NHRCM_NNRP1_GR. Only the values over land are shown for APHRODITE and NHRCM.

g, h). As anticipated, compared with temperature and winds, the simulated rainfall is more strongly affected by the choice of the convective scheme (e.g., see Fersch and Kunstmann 2014). Relative to observed rainfall, the Grell scheme (Figs. 4d, h) has a higher dry bias than that of Kain-Fritsch (Figs. 4c, g). A comparison of runs using the same convective scheme indicates that the boundary condition also affects the spatial distribution and magnitude of rainfall (e.g., Figs. 4c, g), similar to the finding of Park et al. (2013) over Asia.

During DJF, rainfall is high over the eastern coastline of the Philippines. Northeast Mindanao receives up to 25 mm day^{-1} rainfall, while rainfall is about 5–15 mm day^{-1} over the eastern half of the country and lower than 5 mm day^{-1} over the western coast (Figs. 5a, e). Both ERA-Interim and NNRP1 indicate lower rainfall over the east-southeastern coast, while ERA-Interim overestimates rainfall over the southwestern region (Figs. 5b, f). During this season, NHRCM captures the northeast monsoon and generates a rainfall pattern close to that observed with the high rainfall over the southeastern coastline and the drier conditions over the southwest (Figs. 5c, d, g, h). Similar to JJA, the higher dry bias of the Grell scheme (Figs. 5d, h) compared with the Kain-Fritsch scheme (Figs. 5c, g) can be seen over northeast Mindanao during this season. The magnitude and spatial distribution of rainfall are also affected by the choice of boundary condition, such that runs with NNRP1 generate wetter conditions over the eastern coast (e.g., Figs. 5c, g).

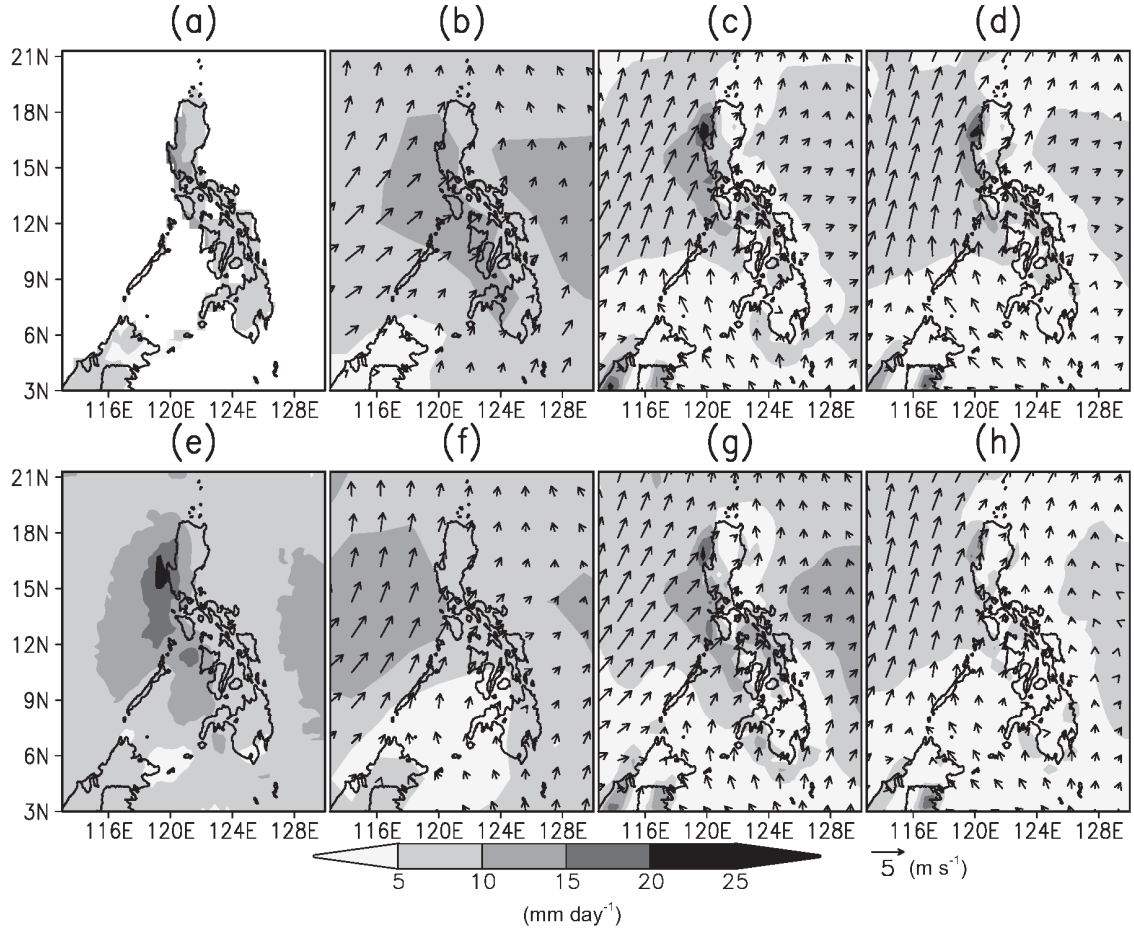

Fig. 4. Average seasonal rainfall (mm day^{-1}) and winds (m s^{-1}) from June to August from (a) APHRODITE (over land only), (b) ERA-Interim, (c) NHRCM_ERA_KF, (d) NHRCM_ERA_GR, (e) TRMM, (f) NNRP1, (g) NHRCM_NNRP1_KF, and (h) NHRCM_NNRP1_GR.

3.2 Regional analysis

a. Temperature

In this section, the performance of NHRCM in simulating temperature is further examined over the five regions defined in Fig. 1. As mentioned in Section 2.2, the simulated temperature is adjusted because of the difference in terrain heights. Since most areas in the model have lower elevation, the model temperature is generally reduced.

The regional 9-year average monthly mean temperature (over land only) in Fig. 6 shows the overall cold bias of the NHRCM model relative to APHRODITE. Differences in the simulated temperature among the model runs tend to be small from June to September but become more notable during the months from January to May, as seen in East Mindanao and Central Visayas. The model performs better in some regions, e.g., East Luzon and West Mindanao, such that deviations tend to be within the observed yearly variability (indicated by the shaded area in each plot of Fig. 6). Despite the bias, NHRCM is able to capture the seasonality in temperature in most regions. In addition, NHRCM has a close but slightly wider distribution compared to APHRODITE, which generates more occurrences of lower temperatures over most of the regions, particularly West Luzon (Fig. 7).

Over West Luzon, NHRCM follows the monthly variation throughout the year and results in correlation values ranging from 0.91 to 0.95 (Fig. 8b). However, the model bias ranges from −1.76°C to −1.33°C across the four experiments (Fig. 8a) because of the

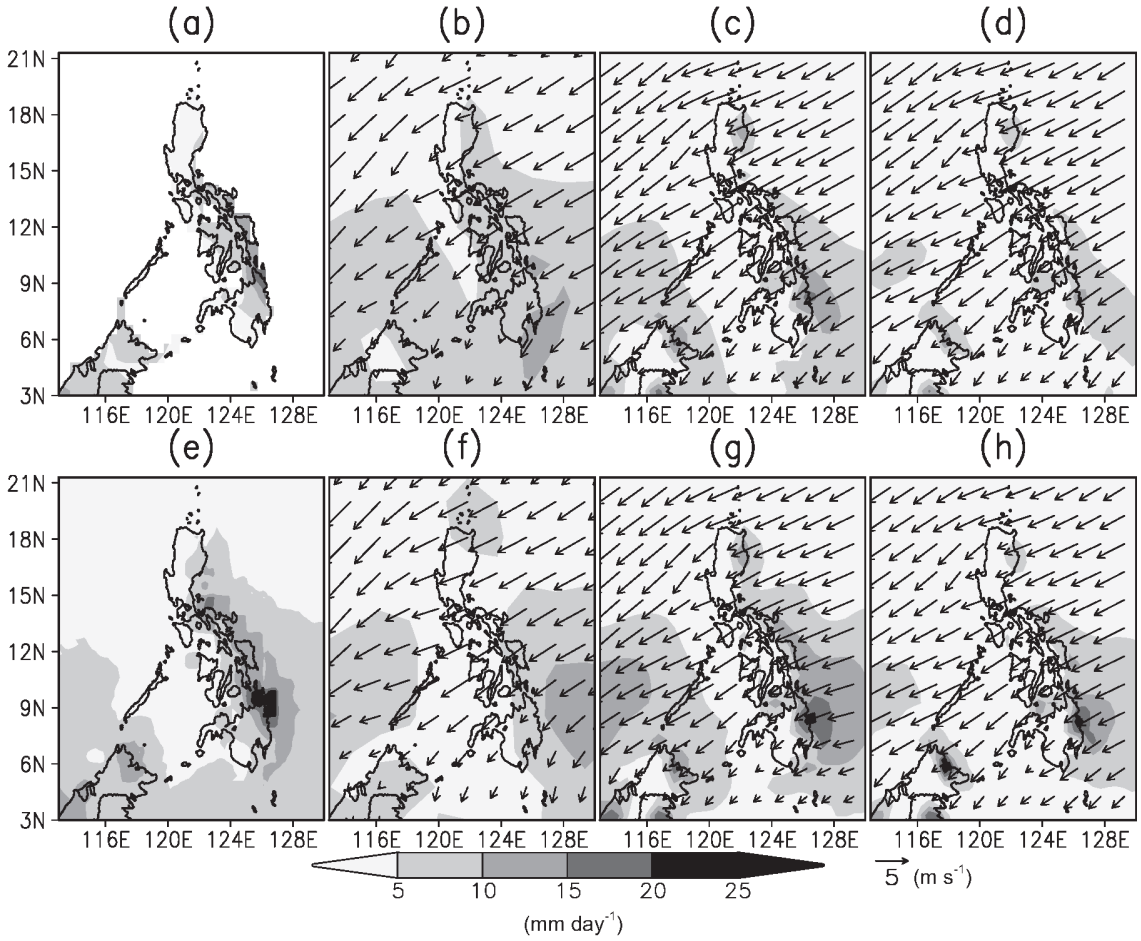

Fig. 5. Average seasonal rainfall (mm day^{-1}) and winds (m s^{-1}) from December to February from (a) APHRODITE (over land only), (b) ERA-Interim, (c) NHRCM_ERA_KF, (d) NHRCM_ERA_GR, (e) TRMM, (f) NNRP1, (g) NHRCM_NNRP1_KF, and (h) NHRCM_NNRP1_GR.

notable underestimation of temperature from August to March. The cold bias is also evident in the probability distribution, wherein the model tends to simulate more months with low temperatures (Fig. 7) and yields an average skill score of 0.70 (Fig. 8c). Among the five regions, NHRCM simulates temperature relatively best in East Luzon (Fig. 8). NHRCM has a lower bias ranging from −0.42°C to 0.07°C in East Luzon (Fig. 8a), with a high average correlation value of 0.95 (Fig. 8b). The probability distribution of the monthly mean temperature also has a high average skill score of 0.93 (Fig. 8c).

The cold bias of NHRCM using ERA-Interim over East Mindanao is lower than that with NNRP1 (Fig. 6). Compared with the other runs, NHRCM_ERA_GR simulates temperature closest to observed, except from June to August, resulting in a low bias of −0.18°C and a high skill score of 0.94 (Fig. 8). The model bias ranges from −1.05°C to −0.51°C in Central Visayas, with relatively high correlation values from 0.82 to 0.93 (Fig. 8). NHRCM_NNRP1_KF yields the highest cold bias (−1.05°C) and the lowest skill score (0.59) as indicated by the deviation of its probability distribution from the observed (Figs. 7 and 8). In West Mindanao, NHRCM has a low bias of −0.23°C, and skill score of 0.88 on average, but the average correlation is moderate (0.68) (Fig. 8).

Comparison of the four experiments over all regions shows the similarity in the seasonal cycle and probability distribution of the simulated temperature when the same convective scheme is used regardless of the boundary condition. There are however differ-

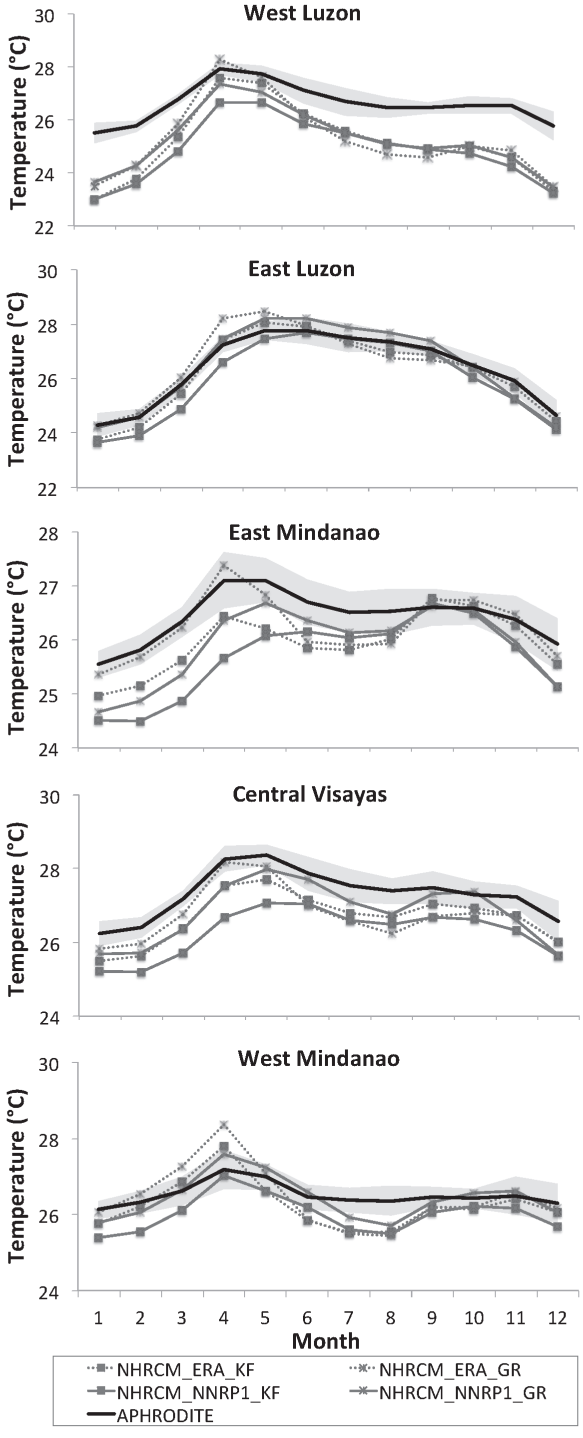

Fig. 6. Monthly mean temperature (°C) from APHRODITE, and NHRCM model, averaged over land in each subregion defined in Fig. 1. Shaded area indicates the year-to-year variation in APHRODITE data. Note that the y-axis may vary for the different subregions.

ences in magnitude depending on the boundary condition such that the temperature bias is lower when using ERA-Interim compared with NNRP1. Fersch and Kunstmann (2014) also showed this influence of the boundary forcing data on the downscaled regional climate. There is a higher correlation over most areas when using the Kain-Fritsch scheme, especially when ERA-Interim is used. On the other hand, using the Grell scheme results in a lower temperature bias and higher skill score.

b. Rainfall

This section examines the skill of NHRCM in simulating rainfall over the five regions (Fig. 1). In general, the seasonality in the 9-year average monthly mean model rainfall is similar with the observed seasonal cycle, but has a tendency to have a dry bias that is outside the yearly variability (indicated by the shaded area in each plot) from May to November (Fig. 9). The dry bias of NHRCM is also reflected in the frequency distribution in Fig. 10, where there are more occurrences of months with total rainfall less than 100 mm in the model compared to those observed.

Figs. 9 and 11 show that NHRCM represents the seasonal rainfall over West Luzon with a relatively high correlation of 0.88 on average. However, the model underestimates the observed peak rainfall in July and has a dry bias ranging from −67.10 % to −32.69 % (Fig. 11a). In East Luzon, NHRCM_NNRP1_KF has a wet bias (15.11 %) as opposed to the dry bias in the other runs (Fig. 11a). NHRCM_ERA_KF and NHRCM_NNRP1_KF have high skill scores (0.84 and 0.92), which is likely due to their ability to capture the heavy rainfall months (Fig. 10).

The deviation in simulated rainfall among the model runs is evident in Central Visayas and East Mindanao (Fig. 9). NHRCM_NNRP1_KF gives the lowest rainfall bias in East Mindanao (−21.34 %) and Central Visayas (−27.34 %) (Fig. 11a). The low dry bias in East Mindanao results from its close simulation of rainfall from January to April, while the other runs simulate relatively drier conditions than observed (Fig. 9). Among the five regions, NHRCM gives the highest dry bias over West Mindanao, ranging from −77.85 % to −59.75 % (Fig. 11a), where monthly mean rainfall does not exceed 10 mm day^{-1}. The underestimation of rainfall over these areas can also be seen in the spatial maps in Figs. 4 and 5.

In general, the model simulations indicate both a higher dry bias with high correlation when ERA-Interim is used, regardless of the convective scheme.

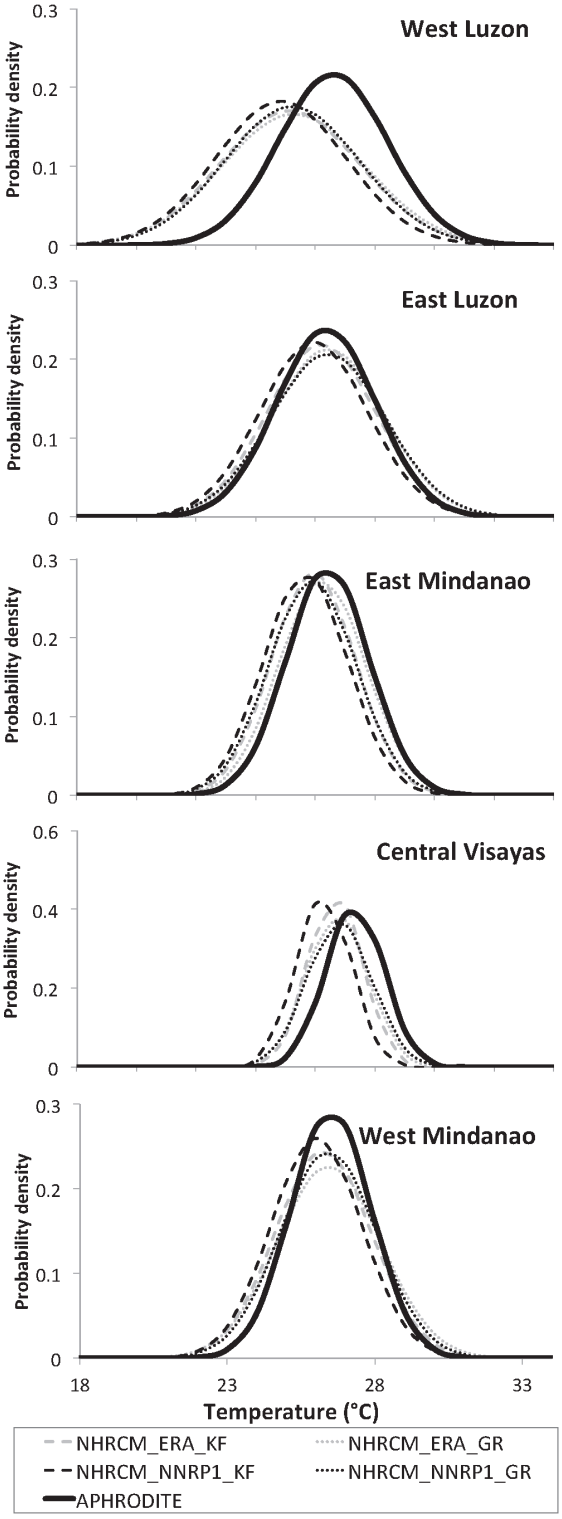

West Luzon	Mean	SD
APHRODITE	26.61	1.84
NHRCM_ERA_KF	25.14	2.34
NHRCM_ERA_GR	25.28	2.40
NHRCM_NNRP1_KF	24.85	2.18
NHRCM_NNRP1_GR	25.23	2.27

East Luzon	Mean	SD
APHRODITE	26.37	1.67
NHRCM_ERA_KF	26.21	1.82
NHRCM_ERA_GR	26.44	1.87
NHRCM_NNRP1_KF	25.95	1.80
NHRCM_NNRP1_GR	26.43	1.93

East Mindanao	Mean	SD
APHRODITE	26.43	1.38
NHRCM_ERA_KF	25.94	1.41
NHRCM_ERA_GR	26.24	1.46
NHRCM_NNRP1_KF	25.67	1.42
NHRCM_NNRP1_GR	25.91	1.47

Central Visayas	Mean	SD
APHRODITE	27.32	0.98
NHRCM_ERA_KF	26.67	0.91
NHRCM_ERA_GR	26.73	1.03
NHRCM_NNRP1_KF	26.27	0.92
NHRCM_NNRP1_GR	26.81	1.09

West Mindanao	Mean	SD
APHRODITE	26.51	1.36
NHRCM_ERA_KF	26.25	1.63
NHRCM_ERA_GR	26.44	1.76
NHRCM_NNRP1_KF	26.01	1.54
NHRCM_NNRP1_GR	26.42	1.64

Fig. 7. Probability density distribution of the monthly mean temperature (°C) from APHRODITE and NHRCM model output over land points within each subregion defined in Fig. 1. Note that the y-axis may vary for the different subregions. Values of the mean and standard deviation are indicated in the tables.

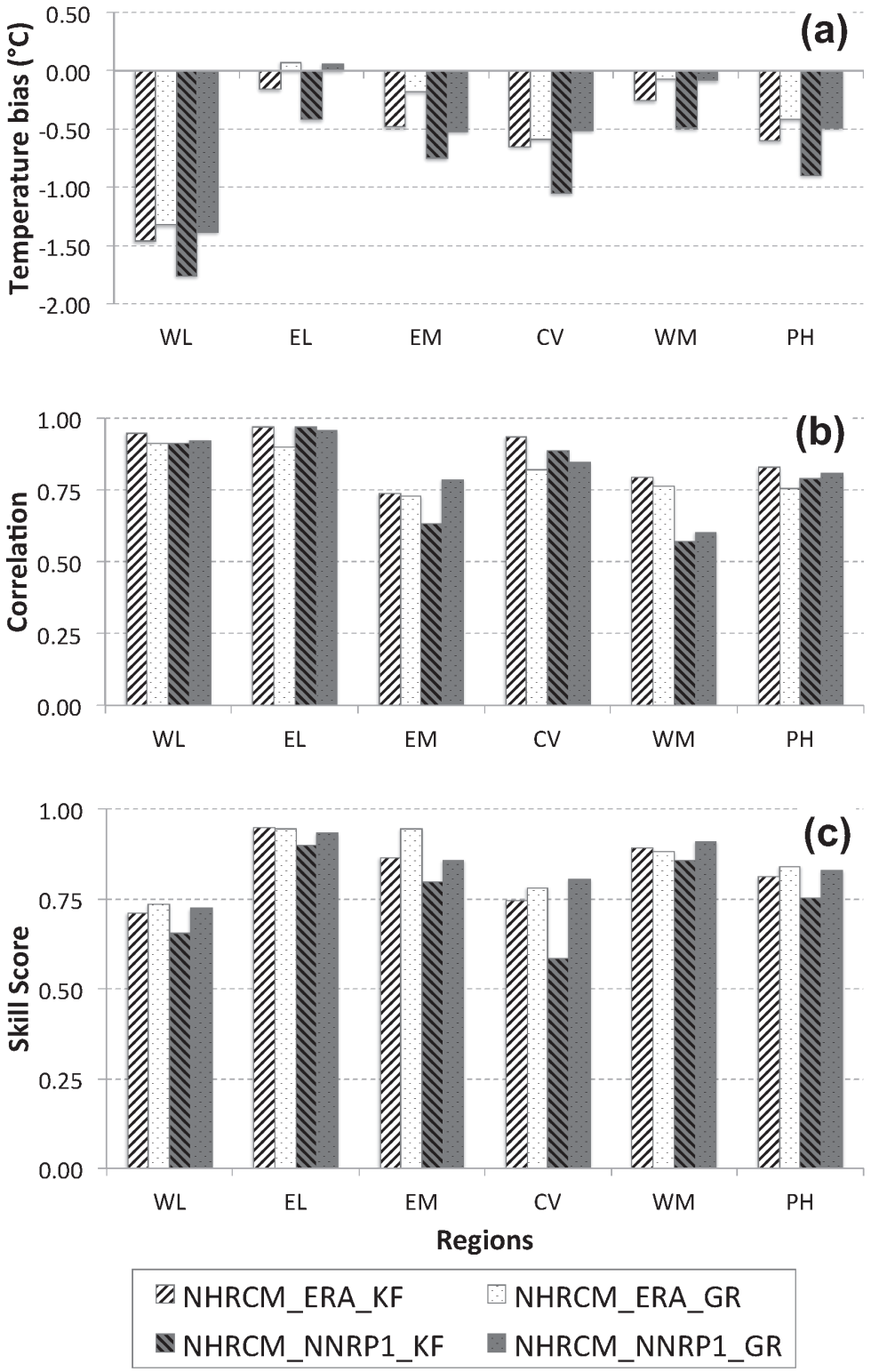

Fig. 8. (a) Bias (units in °C), (b) correlation, and (c) skill score of the model experiments relative to APHRODITE using monthly mean temperature for each subregion, and over the Philippines.

Park et al. (2013) also showed a dry bias in their regional climate simulation over South Korea, but found better results when ERA-Interim was used compared with the NCEP/DOE Reanalysis 2. Using the same boundary condition, the Kain-Fritsch scheme generally has lower dry bias and high correlation and skill scores for rainfall, compared with the Grell scheme (Fig. 11). The influence of the convective scheme on rainfall is also more apparent when NNRP1 is used, particularly during the months with high rainfall (Fig. 9).

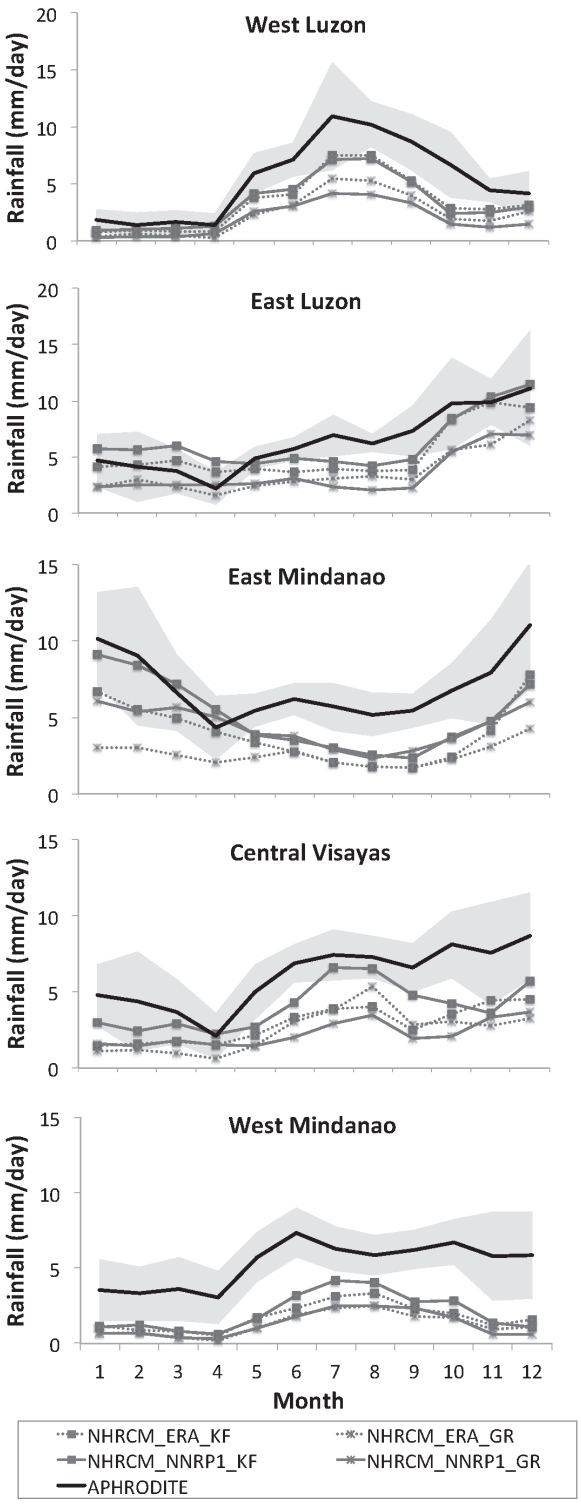

Fig. 9. Monthly mean rainfall (mm day^{-1}) from APHRODITE, and NHRCM model, averaged over land in each subregion defined in Fig. 1. Shaded area indicates the year-to-year variation in APHRODITE data. Note that the y-axis may vary for the different subregions.

4. Concluding remarks

This study examined the applicability of the NHRCM model for simulating the near-recent climate of the Philippines. Simulations were conducted to determine biases and skill of the model, and its sensitivity to the boundary condition and the convective schemes. Results show that the seasonal changes in the spatial distribution of temperature, rainfall, and winds over the Philippines are simulated reasonably well by NHRCM. The regional analyses show that NHRCM has an overall cold and dry bias, wherein the magnitude depends on the boundary condition and choice of convective scheme. Based on the country average, the temperature bias ranges from −0.90°C to −0.42°C (Fig. 8a), while the rainfall bias can be from −62.13 % to −25.20 % (Fig. 11a). Among the simulations conducted, the Grell scheme results in the lowest temperature bias with high skill scores, regardless of the boundary condition. For rainfall, the Kain-Fritsch scheme gives the lowest bias with high correlation and skill scores over most regions and over the country. While NHRCM is able to represent the seasonal cycles of temperature and rainfall, the model tends to produce more occurrences of cold and dry conditions, as indicated in the frequency distribution. Comparison of model runs also indicate the influence of the boundary conditions on the model skill, such that the model tends to have lower temperature bias when ERA-Interim is used, but have lower rainfall bias with NNRP1. In general, NHRCM_ERA_GR performs best for most regions and across the country in terms of temperature, whereas it is NHRCM_NNRP1_KF for rainfall.

There are several limitations in this study that can still be investigated further. Future work can explore the causes of the model biases and the recommenda-

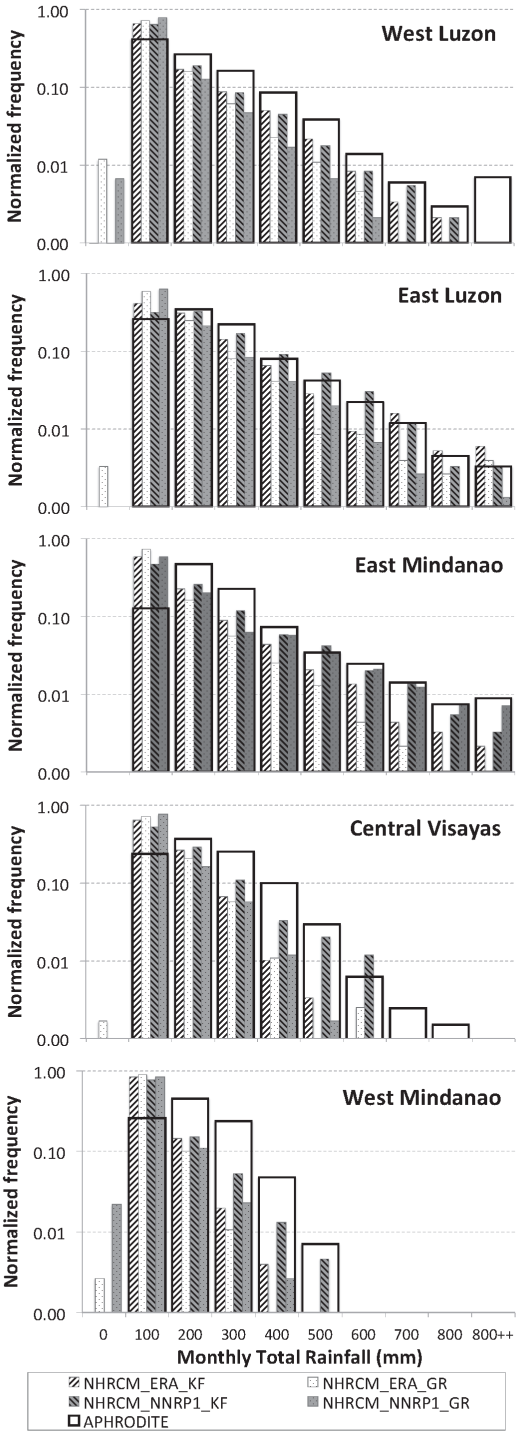

Fig. 10. Frequency distribution of the monthly total rainfall (mm) from APHRODITE, and NHRCM model output over land, normalized with the total number of land points within each subregion defined in Fig. 1 (see Table 2). Note that the y-axis is on a logarithmic scale.

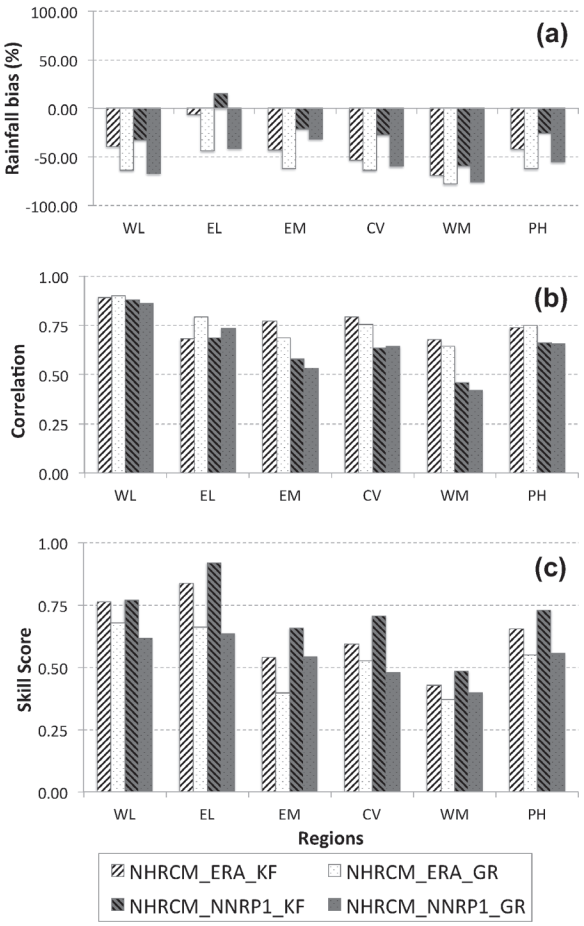

Fig. 11. (a) Bias (units in %), (b) correlation, and (c) skill score of the model experiments relative to APHRODITE using monthly total rainfall for each subregion, and over the Philippines.

tions to reduce them. Fersch and Kunstmann (2014) noted a warm bias in the regional model they used, which was attributed to the skill of the land surface model among other factors. Thus, the contribution of the land surface representation to the model bias can be examined, especially its influence on the energy and water cycles as the spatial resolution becomes higher. These model biases are also relative to the APHRODITE data, which may have its own biases particularly in areas where station data is limited. Differences in the magnitude between the simulated temperature and observed data may also be due to the simulated temperatures obtained at the 1.5 m level.

In this study, the model resolution at 50 km is still relatively coarse for the Philippines. The output needs to be further downscaled to get finer-resolution

climate information necessary for impacts assessment studies. A higher resolution can also better resolve the effects of topography and land use on climate, as well as capture processes at sub-daily timescales. These initial results indicate the potential of the model to be used for historical assessments and to downscale global climate projections to describe future changes in the Philippine climate. The model results can be combined with output from other RCMs to increase the statistical robustness of climate projections for the country. However, further work can still be done to also improve the reproducibility of climate extremes in the model, which is necessary for adaptation planning and risk assessment applications.

Acknowledgment

This work was partly supported by SOUSEI program of the Ministry of Education, Culture, Sports, Science and Technology of Japan. The authors are grateful for the helpful advice and comments from the editors and anonymous reviewers. The authors also thank Dr. Izuru Takayabu for his support on this work, and Dr. Akihiko Murata for his advice.

References

Chotamonsak, C., E. P. Salathé, Jr., J. Kreasuwan, S. Chantara, and K. Siriwitayakom, 2011: Projected climate change over Southeast Asia simulated using a WRF regional climate model. *Atmos. Sci. Lett.*, **12**, 213–219.

Cruz, F. T., G. T. Narisma, M. Q. Villafuerte II, K. U. Cheng Chua, and L. M. Olaguera, 2013: A climatological analysis of the southwest monsoon rainfall in the Philippines. *Atmos. Res.*, **122**, 609–616.

Dee, D. P., S. M. Uppala, A. J. Simmons, P. Berrisford, P. Poli, S. Kobayashi, U. Andrae, M. A. Balmaseda, G. Balsamo, P. Bauer, P. Bechtold, A. C. M. Beljaars, L. van de Berg, J. Bidlot, N. Bormann, C. Delsol, R. Dragani, M. Fuentes, A. J. Geer, L. Haimberger, S. B. Healy, H. Hersbach, E. V. Hólm, L. Isaksen, P. Kållberg, M. Köhler, M. Matricardi, A. P. McNally, B. M. Monge-Sanz, J.-J. Morcrette, B.-K. Park, C. Peubey, P. de Rosnay, C. Tavolato, J.-N. Thépaut, and F. Vitart, 2011: The ERA-Interim reanalysis: configuration and performance of the data assimilation system. *Quart. J. Roy. Meteor. Soc.*, **137**, 553–597.

Fersch, B., and H. Kunstmann, 2014: Atmospheric and terrestrial water budgets: sensitivity and performance of configurations and global driving data for long term continental scale WRF simulations. *Climate Dyn.*, **42**, 2367–2396.

Feser, F., B. Rockel, H. von Storch, J. Winterfeldt, and M. Zahn, 2011: Regional climate models add value to global model data: A review and selected examples. *Bull. Amer. Meteor. Soc.*, **92**, 1181–1192.

Francisco, R. V., J. Argete, F. Giorgi, J. Pal, X. Bi, and W. J. Gutowski, 2006: Regional model simulation of summer rainfall over the Philippines: Effect of choice of driving fields and ocean flux schemes. *Theor. Appl. Climatol.*, **86**, 215–227.

Grell, G. A., 1993: Prognostic evaluation of assumptions used by cumulus parameterizations. *Mon. Wea. Rev.*, **121**, 764–787.

Hirai, M., and M. Oh'izumi, 2004: Development of a new land-surface model for JMA-GSM. 20th Conference on Weather Analysis and Forecasting/16th Conference on Numerical Weather Prediction. [Available at https://ams.confex.com/ams/84Annual/techprogram/paper_68652.htm.]

Huffman, G. J., D. T. Bolvin, E. J. Nelkin, D. B. Wolff, R. F. Adler, G. Gu, Y. Hong, K. P. Bowman, and E. F. Stocker, 2007: The TRMM multi-satellite precipitation analysis (TMPA): Quasi-global, multi year, combined-sensor precipitation estimates at fine scale. *J. Hydrometeor.*, **8**, 38–55.

Im, E.-S., J.-B. Ahn, A. R. Remedio, and W.-T. Kwon, 2008: Sensitivity of the regional climate of East/Southeast Asia to convective parameterizations in the RegCM3 modelling system. Part 1: Focus on the Korean peninsula. *Int. J. Climatol.*, **28**, 1861–1877.

Kain, J. S., and J. M. Fritsch, 1993: Convective parameterization for mesoscale models: The Kain-Fritsch scheme. *The Representation of Cumulus Convection in Numerical Models*. Amer. Meteor. Soc., 165–170.

Kalnay, E., M. Kanamitsu, R. Kistler, W. Collins, D. Deaven, L. Gandin, M. Iredell, S. Saha, G. White, J. Woollen, Y. Zhu, A. Leetmaa, R. Reynolds, M. Chelliah, W. Ebisuzaki, W. Higgins, J. Janowiak, K. C. Mo, C. Ropelewski, J. Wang, R. Jenne, and D. Joseph, 1996: The NCEP/NCAR 40-year reanalysis project. *Bull. Amer. Meteor. Soc.*, **77**, 437–471.

Kida, H., T. Koide, H. Sasaki, and M. Chiba, 1991: A new approach for coupling a limited area model to a GCM for regional climate simulations. *J. Meteor. Soc. Japan*, **69**, 723–728.

Kistler, R., W. Collins, S. Saha, G. White, J. Woollen, E. Kalnay, M. Chelliah, W. Ebisuzaki, M. Kanamitsu, V. Kousky, H. van den Dool, R. Jenne, and M. Fiorino, 2001: The NCEP–NCAR 50–year reanalysis: Monthly means CD–ROM and documentation. *Bull. Amer. Meteor. Soc.*, **82**, 247–267.

Nakano, M., T. Kato, S. Hayashi, S. Kanada, Y. Yamada, and K. Kurihara, 2012: Development of a 5-km mesh cloud-system-resolving regional climate model at the Meteorological Research Institute. *J. Meteor. Soc. Japan*, **90A**, 339–350.

Ohmori, S., and Y. Yamada, 2004: Implementation of the Kain–Fritsch convective parameterization scheme in the JMA's non-hydrostatic model. *CAS/JSC WGNE Res. Activ. Atmos. Oceanic Modell.*, **34**, 425–426.

PAGASA, 2011: *Climate Change in the Philippines*. Funded by the MDGF 1656: Strengthening the Philippines' Institutional Capacity to Adapt to Climate Change Project. DOST-PAGASA, 85 pp.

Park, J.-H., S.-G. Oh, and M.-S. Suh, 2013: Impacts of boundary conditions on the precipitation simulation of RegCM4 in the CORDEX East Asia domain. *J. Geophys. Res.*, **118**, 1652–1667.

Perkins, S. E., A. J. Pitman, N. J. Holbrook, and J. McAneney, 2007: Evaluation of the AR4 climate models' simulated daily maximum temperature, minimum temperature, and precipitation over Australia using probability density functions. *J. Climate*, **20**, 4356–4376.

Roberts, M. G., D. Dawe, W. P. Falcon, and R. L. Naylor, 2009: El Niño-Southern Oscillation impacts on rice production in Luzon, the Philippines. *J. Appl. Meteor. Climatol.*, **48**, 1718–1724.

Robertson, A. W., J.-H. Qian, M. K. Tippett, V. Moron, and A. Lucero, 2012: Downscaling of seasonal rainfall over the Philippines: Dynamical versus statistical approaches. *Mon. Wea. Rev*., **140**, 1204–1218.

Saito, K., T. Fujita, Y. Yamada, J. Ishida, Y. Kumagai, K. Aranami, S. Ohmori, R. Nagasawa, S. Kumagai, C. Muroi, T. Kato, H. Eito, and Y. Yamazaki, 2006: The operational JMA nonhydrostatic mesoscale model. *Mon. Wea. Rev.*, **134**, 1266–1298.

Sasaki, H., Y. Sato, K. Adachi, and H. Kida, 2000: Performance and evaluation of the MRI regional climate model with the spectral boundary coupling method. *J. Meteor. Soc. Japan*, **78**, 477–489.

Sasaki, H., K. Kurihara, I. Takayabu, and T. Uchiyama, 2008: Preliminary experiments of reproducing the present climate using the non-hydrostatic regional climate model. *SOLA*, **4**, 25–28.

Sasaki, H., A. Murata, M. Hanafusa, M. Oh'izumi, and K. Kurihara, 2011: Reproducibility of present climate in a non-hydrostatic regional climate model nested within an atmosphere general circulation model. *SOLA*, **7**, 173–176.

Silang, A., S. N. Uy, J. M. Dado, F. A. Cruz, G. Narisma, N. Libatique, and G. Tangonan, 2014: Wind energy projection for the Philippines based on climate change modeling. *Energy Procedia*, **52**, 26–37.

Villafuerte, M. Q., J. Matsumoto, I. Akasaka, H. G. Takahashi, H. Kubota, and T. A. Cinco, 2014: Long-term trends and variability of rainfall extremes in the Philippines. *Atmos. Res.*, **137**, 1–13.

Villarin, J. T., and G. T. Narisma, 2011: Endangered Climate. *Stellar Origins, Human Ways. Readings in Science, Technology and Society*. Cuyegkeng, M. A. C. (ed.), Ateneo de Manila University Press, Quezon City, Philippines, 211–229.

Wei, Y., S.-K. Santhana-Vannan, and R. B. Cook, 2009: Discover, visualize, and deliver geospatial data through OGC standards-based WebGIS system. *Geoinformatics, 2009 17th International Conference on*. IEEE, 1–6.

Yamada, Y., 2003: Introduction to the Kain–Fritsch scheme. *Separate volume of annual report of Numerical Prediction Division*. Japan Meteorological Agency, **49**, 84–89 (in Japanese).

Yasunaga, K., H. Sasaki, Y. Wakazuki, T. Kato, C. Muroi, A. Hashimoto, S. Kanada, K. Kurihara, M. Yoshizaki, and Y. Sato, 2005: Performance of long-term integrations of the Japan Meteorological Agency nonhydrostatic model using the spectral boundary coupling method. *Wea. Forecasting*, **20**, 1061–1072.

Yasutomi, N., A. Hamada, and A. Yatagai, 2011: Development of a long-term daily gridded temperature dataset and its application to rain/snow discrimination of daily precipitation. *Global Environ. Res.*, **15**, 165–172.

Yatagai, A., O. Arakawa, K. Kamiguchi, H. Kawamoto, M. I. Nodzu, and A. Hamada, 2009: A 44-year daily gridded precipitation dataset for Asia based on a dense network of rain gauges. *SOLA*, **5**, 137–140.

Yatagai, A., K. Kamiguchi, O. Arakawa, A. Hamada, N. Yasutomi, and A. Kitoh, 2012: APHRODITE: Constructing a long-term daily gridded precipitation dataset for Asia based on a dense network of rain gauges. *Bull. Amer. Meteor. Soc.*, **93**, 1401–1415.